Journal of the Korean Ceramic Society (2020) 57:503–512
https://doi.org/10.1007/s43207-020-00052-x

ORIGINAL ARTICLE

Effect of heat-treatment temperature on mechanical properties and microstructure of alumina–SiC nanocomposite

Amir Fathi[1] · **Hamidreza Baharvandi**[2]

Received: 26 October 2019 / Revised: 20 January 2020 / Accepted: 27 January 2020 / Published online: 20 May 2020
© The Korean Ceramic Society 2020

Abstract
In this investigation, 90 vol. % alumina and 10 vol. % silicon carbide nanopowders were combined. Initial samples were fabricated by the hot press method under 20-MPa pressure of 1650 °C. Then, the nanocomposites were heat-treated at 1200, 1400, 1500, and 1600 °C for several hours. After the heat-treatment, XRD (X-ray diffraction), SEM (scanning electron microscope), and FE-SEM (field emission scanning electron microscope) analyses were used to explore the nanocomposite specifications and microstructure. The flexural strength, apparent density, crack healing, and fracture toughness were measured to study the physical and mechanical properties of nanocomposite specimens. The best result for flexural strength was achieved for specimens heat-treated at 1500 °C for 2 h, exhibiting a 34% increase in the flexural strength. Furthermore, with heat-treatment at 1600 °C for 2 h, the fracture toughness for nanocomposite reached 5.563 MPa $m^{1/2}$.

Keywords Alumina · SiC · Nanocomposite · Heat-treatment

1 Introduction

Remarkable efforts have in recent years been devoted to the development of mechanical properties of ceramic matrix composite materials reinforced with a second phase in the form of particles, whiskers, fibers, etc. [1–3]. Generally, ceramic nanocomposites are classified into three categories: (a) ceramic–ceramic nanocomposites, (b) ceramic–metal nanocomposites, and (c) polymer–ceramic nanocomposites. Ceramic–ceramic nanocomposites are comprised of two inorganic ceramic phases that differ in their mechanical and thermal properties. In this type of nanocomposite, the ceramic field is reinforced by another ceramic phase with nanosize dimensions [4].

Alumina is a technical ceramic that is extensively used across different industries owing to its high-temperature strength, hardness, chemical stability, and high thermal and electrical insulating performances [5]. These properties have made alumina a suitable candidate for applications in various fields, including high-temperature applications, dental implants, wear-resistant parts, thermal insulators, and high-speed cutting tools [6]. However, the brittleness of alumina, as one of its inherent properties, has restricted its use in various applications. This motivated efforts to improve its fracture toughness [7].

Alumina-based composites and nanocomposites, which are created through the addition of suitable second phase nanoparticles or fibers, can exhibit improved mechanical and functional performance compared to alumina. Several materials, such as titanium carbide (TiC), zirconia (ZrO_2), titanium nitrite (TiN), and silicon carbide (SiC), have been used to reinforce alumina [8–11].

Al_2O_3/SiC nanocomposites have been extensively studied because of the reported remarkable improvement of their mechanical properties, namely fracture strength, both at room and at high temperatures, in comparison to monolithic alumina [1]. Addition of small amounts of sub-micron SiC particles to polycrystalline alumina was reported to significantly improve hardness, fracture strength, and fracture toughness [7, 12–14]. Furthermore, in most studies, MgO nanoparticles are added to the Al_2O_3/SiC nanocomposite mixture, as they contribute the most significant, including a

✉ Amir Fathi
a-fathi@tvu.ac.ir

Hamidreza Baharvandi
baharvandee@yahoo.com

[1] Material Engineering Department, Technical and Vocational University, Mianeh, Iran

[2] Material Engineering Department, Maleke Ashtar University of Technology, Tehran, Iran

decrease in the grain boundary mobility, increased surface diffusion, and decline of the grain anisotropy [15].

For the fabrication of nanocomposites, after preparing primary nanopowders by the ball mill method, one of the crucial steps in the production of alumina–SiC nanocomposites is sintering. Fundamentally, there are several methods for the generation of alumina–SiC nanocomposites, such as sintering in the presence of the liquid phase, plasma method, hot press, and non-pressure method. In this investigation, sintering without pressure and the hot press method are explored and described.

The pressurizing process that is part of the pressurized methods is cold, which could be the reason behind the multiple-step pressure operations. In contrast, the hot press (HP) method requires more time, as well as a higher temperature and pressure. For these types of methods to execute the suitable manufacture of nanocomposites at low pressures, a higher temperature is required. Timms and his colleagues employed this method to synthesize Al_2O_3–SiC nanocomposite bodies [16].

The HP method is the most common and expensive procedure that is used to synthesize ceramic base composites. Other methods are typically significantly more difficult. Furthermore, ceramic composites produced by the HP have superior quality and reduced thermal incompatibility between primary components. For example, Wang and his colleagues produced 5% SiC–95%Al_2O_3 nanocomposites at the pressure of 30 MPa and temperatures from 1600 to 1800 °C for 1 h in a nitrogen atmosphere [17]. Moreover, researchers have reported that composites containing 5 wt % and 10 wt % SiC nanoparticles in the alumina matrix exhibit the best mechanical performances compared to other composites [18, 19].

After the production of Al_2O_3–SiC nanocomposites, one of the most important ways to improve mechanical properties such as flexural strength and fracture toughness is heat-treatment. Therefore, the present study sets out to investigate this procedure at various temperatures and times after the synthesis of nanocomposites by the HP method.

Conveniently, the flexural strength of defective ceramics is restored by heat-treatment. In this case, the improvement of strength is associated with the following reasons: release of remaining tensile stress, re-sintering defects, and restoration of cracks. Regarding the Al_2O_3 and Al_2O_3–SiC composite, the release of tensile stress and re-sintering procedures in vacuum, nitrogen, argon, and air atmosphere is achievable [20]. However, crack restoration is not achievable in a vacuum, nitrogen, and argon atmosphere, because crack restoration is possible through the following reaction:

$$SiC + \frac{3}{2}O_2 \rightarrow SiO_2 + CO + 943 \text{ KJ/mol}$$

To complete the crack restoration reaction, O_2 is essential. To achieve these conditions and the best state, SiC nanosize particles should be added by more than 10 vol. % in composite. Ando and colleagues proposed a reliable method to manage the life of ceramic parts using crack restoration [20]. Kim et al. investigated the effect of annealing on SiC–alumina nanocomposites. In this study, sintered SiC–Al_2O_3 had a grain size of about 1 μm and a relative density of about 99%. Some SiC nanoparticles are distributed among Al_2O_3 grains and some others inside the Al_2O_3 grains. After sintering and preparation of samples, cracks were created by the Vickers indenter using a load of 24.5 N. Regular and accurate crack repair was evaluated as a function of the crack repair temperature (1273–1723 °C) for 1 h in air [21].

1.1 Experimental procedure

Primary materials were used in recent research, including 90 vol. % of pure gamma-alumina nanopowders (99.9%, ≤ 20 nm size), 10 vol. %, of SiC nanoparticles (99% and ≤ 80 nm size), and magnesium oxide nanopowders (98% and less than 100 nm size). The concentration of magnesium oxide nanopowder was 500 ppm compared to the solid weight of the composite specimen. The raw materials were mixed with a high-power ball mill with tungsten carbide balls in isopropanol solution at 150 rpm for 3 h. The solution exiting the ball mill was dried for 24 h at 90 °C in the oven. The dried mixture was shaped by a hydraulic-press into rectangular shapes. These shaped samples were sintered by the HP device at 1650 °C for 2 h in Ar atmosphere at about 20-MPa pressure, where the rate of increasing temperature was 8 °C/min. Subsequently, nanocomposite samples were annealed in the heat-treatment furnace at 1200, 1400, 1500, and 1600 °C for 1, 2, and 3 h, and the increasing rate of furnace temperature was 5 °C/min. After heat-treatment, the furnace turned off, and specimens were cooled at the furnace atmosphere.

Mechanical and structural properties of nanocomposites (crack restoration, flexural strength, density, fracture toughness, and microstructure at various temperatures and times) were investigated. X-ray diffraction was used to study phases after the heat-treatment. The Vickers method was used to create controlled-size cracks at surfaces of nanocomposites to probe crack improvement and its restoration. To this end, composite samples were machined using diamond blades to desired dimensions according to standard B samples. Then, samples were sanded using a diamond plate and subsequently polished with a 30, 6, and 1 μm pulp. The dimensions of the standard B sample are 45-mm height, 4-mm width, 3-mm thickness. The apparent density of nanocomposites was examined using the Archimedes method with the ASTM B311-17 method. Employing this method, samples were dried at 110 °C for 24 h, and the dried sample weight was used to calculate the apparent density [22]. To measure the flexural strength of manufactured composites,

first they were cut and ground into rectangular specimens (4×3×45 mm), and subsequently they were loaded according to ASTM-C1161 [23]. The fracture toughness of nanocomposites after heat-treatment was analyzed. The nanocomposite surfaces were probed by the scanning electron microscope (SEM). X-ray diffraction (XRD) analysis was used to explore attained phases of composites before and after heat-treatment. To investigate the structure, SEM and field emission scanning electron microscope (FE)-SEM methods were used to study the microstructure and line sectioning of samples.

2 Results and discussion

2.1 Crack healing

The healing of cracks in Al_2O_3–SiC nanocomposites was a prominent factor investigated in this study. During the heat-treatment procedure, more nanocomposite cracks could be removed. For a better investigation, some Vickers cracks were created in composites. Therefore, an annealing (heat-treatment) process after the primary sintering process was required to restore mechanical properties.

Since machining cracks were hardly visible, some primitive cracks were induced by the Vickers method. In this method, several controlled cracks were created on the surface of nanocomposites. Vickers indentation was used to create radial cracks on composite surfaces, which can easily be seen under the microscope. Figure 1a shows SEM images of Vickers method cracks. Figure 1b illustrates SEM images of samples after annealing at 1400 °C for 1 h. The optimum temperature for crack restoration was determined according to the results of flexural strength tests. After annealing, Vickers method cracks were completely removed (Fig. 1). The thickness of Vickers effect cracks was about 0.5 µm, which were repaired and healed by heat-treatment (annealing).

To better understand crack repair, the mechanism is illustrated in Fig. 2 [23]. The main reaction for crack restoration is the following oxidation:

$$SiC + O_2 \rightarrow SiO_2 + CO(CO_2)$$

Oxygen reacts with silicon carbide and forms SiO_2. SiO_2 is a glass and crystalline phase that has some suitable properties such as high thermal resistance and high-thermal strength [24]. The crack healing was attributed to strong bonding by the glass phase on the surface environment of alumina–SiC nanocomposites [24].

2.2 XRD results

Figure 3 shows XRD patterns of the nanoalumina/nanoSiC composite before heat-treatment. Alumina

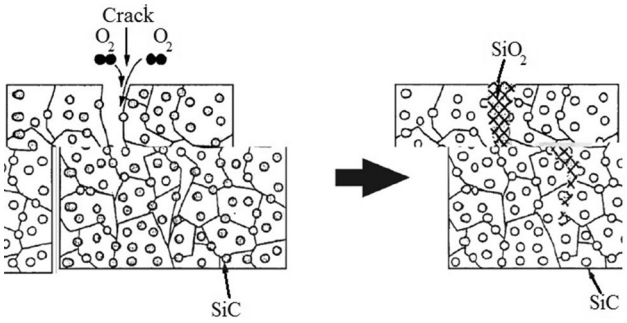

Fig. 2 Mechanism of crack healing by SiO_2 [22]

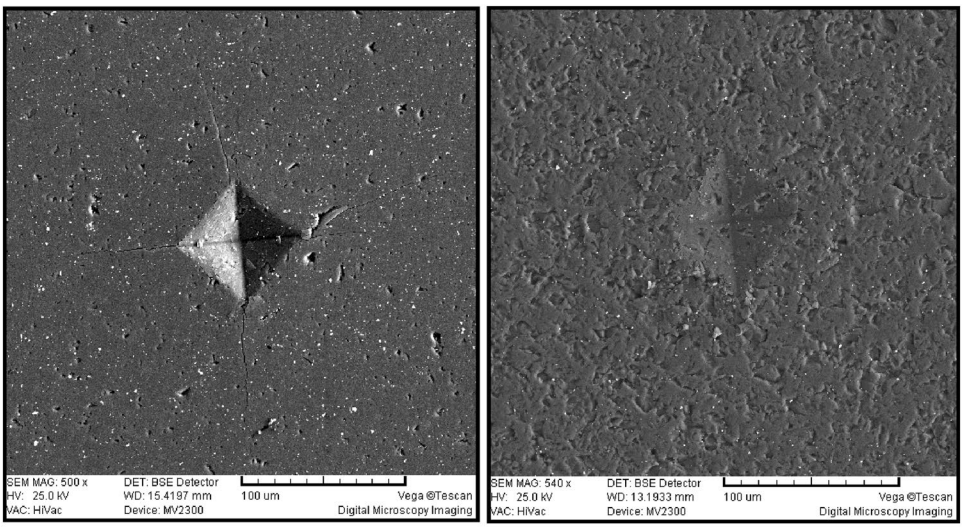

Fig. 1 **a** SEM image of alumina-SiC nanocomposite; **b** SEM image of composite after heat-treatment

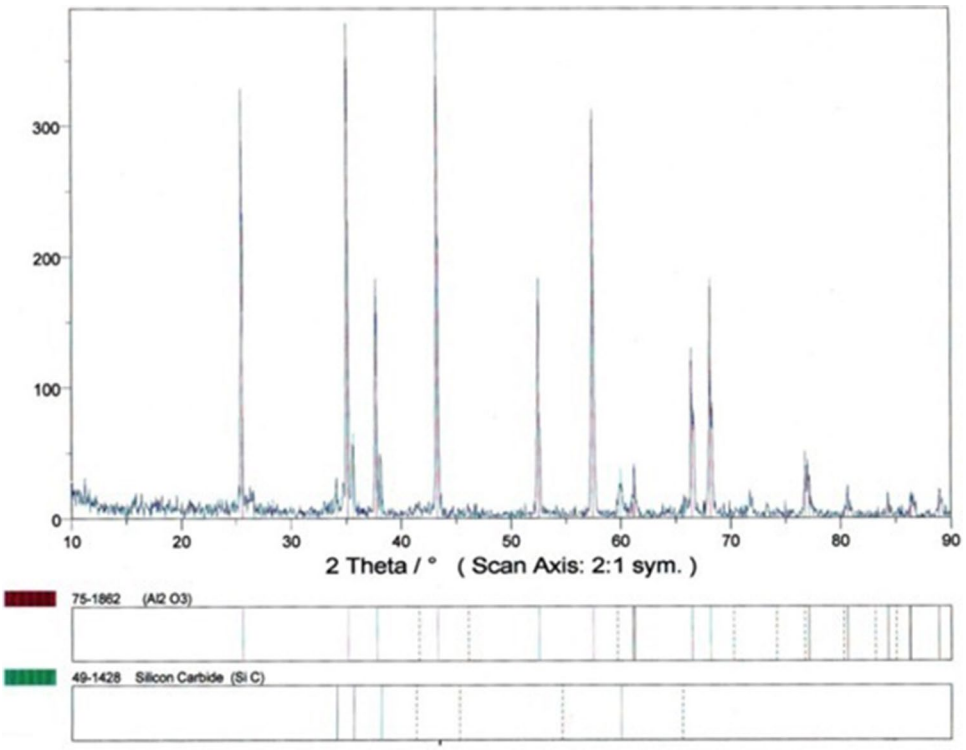

Fig. 3 XRD results for alumina–SiC nanocomposite

and silicon carbide peaks were detected. Figure 4 presents XRD patterns of nanoAl_2O_3/nanoSiC composite after annealing at 1500 °C for 2 h. XRD patterns of the resultant heat-treated nanocomposite comprised mullite ($3Al_2O_3.2SiO_2$), alumina, SiC, and SiO_2. The presence of mullite and SiO_2 indicates a surface reaction between SiC and Al_2O_3 powders.

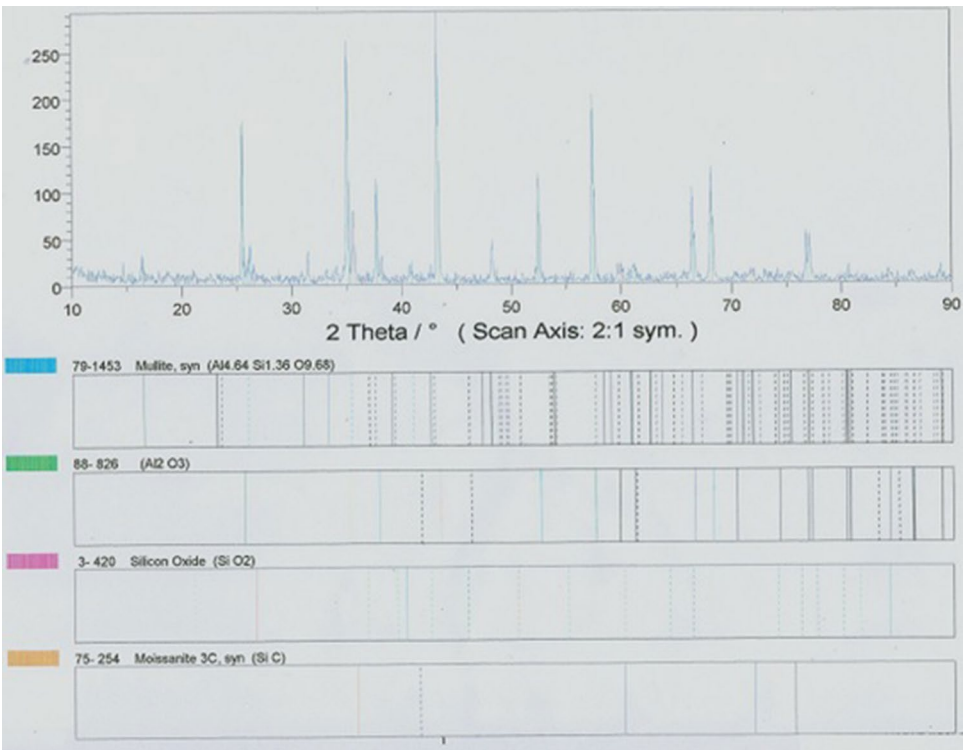

Fig. 4 XRD results for alumina–SiC nanocomposite after heat-treatment at 1500 °C for 2 h

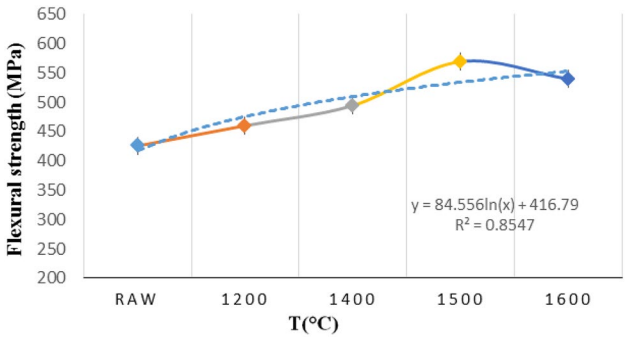

Fig. 5 Diagram of flexural strength for nanoalumina–nanosilicon carbide nanocomposites without heat-treatment and with heat-treatment at 1200, 1400, 1500, 1600 °C for 2 h

2.3 Flexural strength

Figure 5 illustrates the trend of flexural strength for nanocomposites without heat-treatment and after heat-treatment at various temperatures for 2 h.

According to the results from Fig. 5, with an increasing temperature of heat-treatment from 1200 to 1500 °C for 2 h, the flexural strength was raised significantly. The highest flexural strength was measured after the heat-treatment at 1500 °C, which was about 569 MPa. This value of the flexural strength was acceptable when compared with other research results [12, 17]. Therefore, the heat-treatment has had a considerable effect on the strength of nanocomposites. The upgrading of flexural strength can be explained by crack improvement after heat-treatment, which led to a decline in the density of structural defects, and thus the critical crack size was decreased.

The flexural strength of raw materials was determined within 425 MPa. The maximum flexural strength in heat-treated samples at 1500 °C for 2 h was measured at 569 MPa, which yielded a 34% increase compared to the primary nanocomposite without heat-treatment. This striking rise in flexural strength was associated to crack healing, which improves mechanical properties and reduces surface defects. Moreover, the oxidation of SiC particles in air atmosphere during heat-treatment had a positive effect on the improvement of cracks, hence this reaction had an excellent impact on upgrading mechanical properties. Declining flexural strength at temperatures above 1500 °C could be related to the grain size. With increasing heat-treatment temperature, the grain growth was increased, which decreases flexural strength. (The growth of grain size with increasing annealing temperature was demonstrated in Fig. 10 at the microstructure section).

After sintering, when composites are cooled, residual stresses remained in the matrix. Residual stresses can result in the formation of micro-cracks, which themselves could cause crack branching and stress relaxation near the crack tips in composites. The heat-treatment process had an impressive impact on the enhancement of mechanical properties of alumina–SiC nanocomposites [25, 26]. Further, after studying flexural strength at various heat-treatment duration (1, 2, and 3 h), a suitable and acceptable time of around 2 h was achieved.

2.4 Fracture toughness

In Fig. 6, the effect of the heat-treatment temperature on fracture toughness at various temperatures for nanocomposites (nanoalumina/nanoSiC) is shown. Examinations and calculations for this investigation were performed according to the Anstis method.

Given the fracture toughness results for nanocomposites after heat-treatment at various temperatures, the fracture toughness amount increases from 1200 to 1600 °C. Such remarkable fracture mode quantities were achieved particularly after heat-treatment at 1500 °C and 1600 °C for 2 h. The fracture toughness at 1500 °C reached 5.5 Mpa $m^{1/2}$, and at 1600 °C it reached 5.563 MPa $m^{1/2}$. These results are very close together, therefore, the optimum heat-treatment is considered to be around 1500 °C.

In this study, the important reason to improve fracture toughness was related to crack deviation, which causes the expansion of tensile fields around SiC particles, which was intensified with the difference in the thermal expansion coefficient between the secondary phase particles and base phase of the composite. Generally, the crack deviation acted in the crack-head. Upon crack growth, the path of the crack reached the second phase, and the primary crack plane deviated to a new plane, which constitutes the mechanism of crack deviation. Observations in electron microscopy images show that the crack deviation in alumina–SiC nanocomposites has a direct relationship with silicon carbide nanoparticles and micro-cracks in the body of the nanocomposite, which these caused to promote fracture toughness.

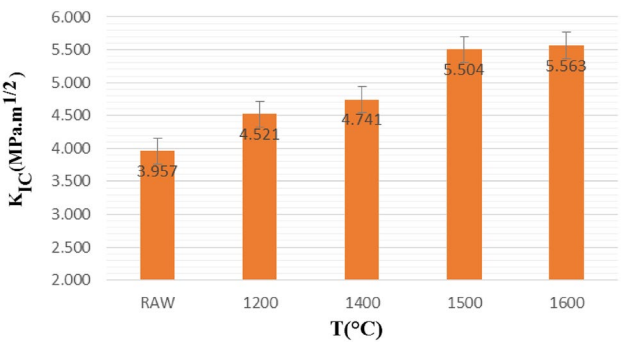

Fig. 6 Chart of fracture toughness results for alumina-SiC nanocomposite before and after heat-treatment at various temperatures for 2 h

Table 1 Previous studies on fracture toughness of Alumina–SiC nanocomposite [16, 18, 26–28]

Volume fraction of alumina–SiC	Synthesis method	Fracture toughness (MPa $m^{1/2}$)	Researchers
Al_2O_3–10%SiC	SHS*	4.4	Johnson et al. [27]
Al_2O_3–5%SiC	HP	4.7	Wang et al. [17]
Al_2O_3–5%SiC	HP	2.9	Sciti et al. [19]
Al_2O_3–5%SiC	HP	4.7	Sun et al. [28]
Al_2O_3–5%SiC	SHS	2.65	Saheb et al. [19]

*Spark plasma sintering

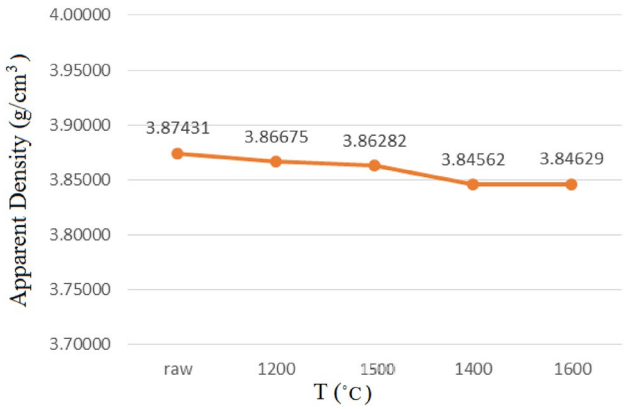

Fig. 7 Diagram of apparent density of nanocomposites after heat-treatment at various temperatures for 2 h

By comparing the results of previous studies, we found that the heat-treatment of alumina–SiC nanocomposite significantly increased fracture toughness. Previous studies on fracture toughness are shown in Table 1, whose values present a considerable effect of heat-treatment on the fracture toughness of alumina–SiC nanocomposite [17, 19, 27–29].

2.5 Apparent density

Figure 7 presents the effect of heat-treatment temperature from 1200 to 1600 °C for 2 h on the apparent density of alumina/SiC nanocomposite specimens. According to this figure, the trend of apparent density within heat-treatment temperatures was declining slightly, and at 1500 °C and 1600 °C it reached a steady value of about 3.84 g/cm^3.

Results in Fig. 7 indicate that heat-treatment slowly decreases the apparent density. With the rising temperature in the heat-treatment operation, the density maintains its decreasing trend. The density reduction in heat-treated nanocomposites can be related to the evaporation of gas products of ongoing reactions and formation of low-density phases, such as mullite (3.16 g/cm^3) and SiO_2 (2.56 g/cm^3).

2.6 FE-SEM and map analysis

Figure 8a illustrates the line scan from the FE-SEM image of the alumina/SiC nanocomposite after heat-treatment at 1500 °C for 2 h at a distance of 150 µm below the surface. The results obtained from the line scan are shown in Fig. 8b, c, and d. After the investigation of linear scanning, it was concluded that the oxygen content in the surface was remarkable compared to other regions; thus, the thickness of the oxide layer could be estimated within 10 µm.

The oxygen content at the surface of the nanocomposite is shown in the map method analysis of Fig. 9, which presents a detailed map image of the nanocomposite after heat-treatment at 1500 °C for 2 h at a distance of 30 µm below the surface. In this image (Fig. 9d), it can be clearly seen that the oxygen dispersion (white points) was not monotonous across the entire of specimen, and there was a higher oxygen content on the surface of nanocomposite, which this is a positive sign of complete oxidizing reactions at the surface of the nanocomposite after the heat-treatment process. In contrast, Figs. 9b and c show that the dispersion of Al and Si elements in entire map images is more uniform than oxygen.

2.7 Microstructure study

Figure 10 illustrates SEM images of the alumina–SiC nanocomposite after heat-treatment at 1400 °C and 1500 °C for 2 h. The analysis of SEM images shows that white regions contain more oxygen than other regions. Further, by increasing the annealing temperature, white areas were increased. The higher concentration of oxygen at surface areas indicates the existence of silicon oxide and mullite phases on the surface of nanocomposites after heat-treatment.

3 Conclusions

Finally, the results of heat-treatment on alumina–SiC nanocomposite samples are associated with the improvement in the mechanical properties of nanocomposites, and other conclusions were related to microstructure specifications. First, heat-treatment affects nanocomposites to generate new phases, such as mullite and silicon dioxide. These were formed by a surface reaction between alumina and silicon carbide, improving mechanical properties such as flexural strength and crack-healing as well. These compositions after heat-treatment are assumed to be a significant achievement in the growth of specifications of alumina–SiC nanocomposites. Further, newly synthesized phases could penetrate among nanocomposite porosities and cause heightened resistance against crack growth. The XRD analysis depicts several phases, including alumina, silicon carbide, mullite, and silicon oxide, demonstrating the generation of these

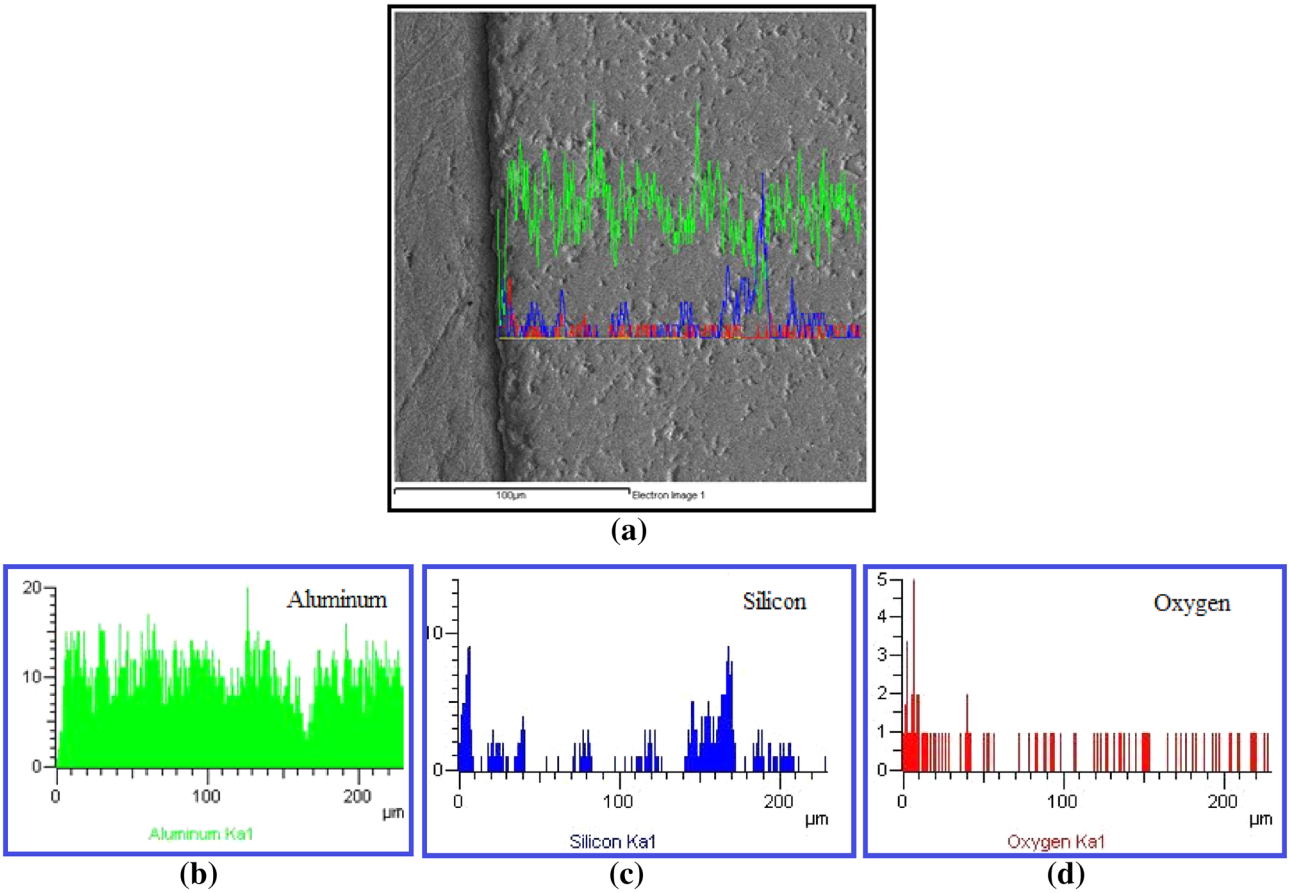

Fig. 8 FE-SEM image (**a**) and line scans results (**b**, **c**, and **d**) of alumina/SiC nanocomposite after heat-treatment at 1500 °C for 2 h

products. Reviewing the density of nanocomposites, it can be seen that there was a slight decline in the apparent density for samples. This might pertain to the production of gas crops, such as silicon oxides, at high temperatures. Moreover, one of the striking results of this research is related to the effect of heat-treatment on the nanocomposites' flexural strength property. The flexural strength values after heat-treatment increased considerably at temperatures close to 1500 °C after 2 h, reaching about 568 MPa. This result presents an impressive effect after heat-treatment for the alumina–SiC nanocomposite. At temperatures above 1500 °C, due to growing grain sizes and surface destruction, the flexural strength and other mechanical properties generally deteriorated. Furthermore, the fracture toughness was investigated after the heat-treatment process. The results show that with the heat-treated nanocomposite at 1500 °C and 1600 °C, there was a considerable increase in the fracture toughness, measured at about 5.5 MPa $m^{1/2}$. After comparison to previous studies, this value seems acceptable. Finally, by SEM and FE-SEM image analysis of heat-treated specimens at 1500 °C for 2 h, remarkable crack repair is observed in the nanocomposites, which indicates a significant improvement for mechanical properties of alumina–SiC nanocomposites.

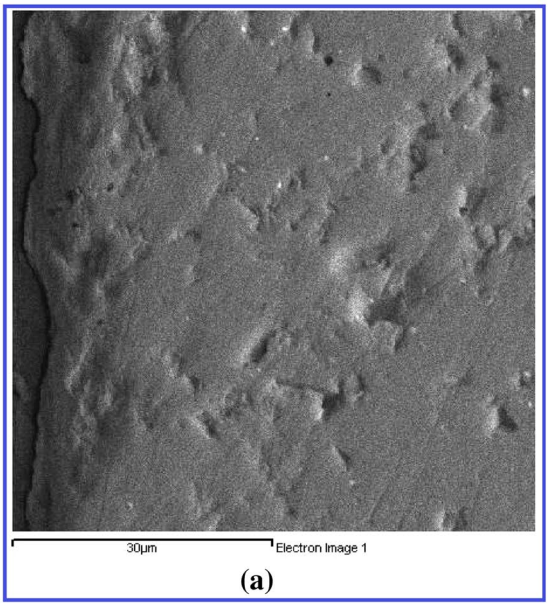

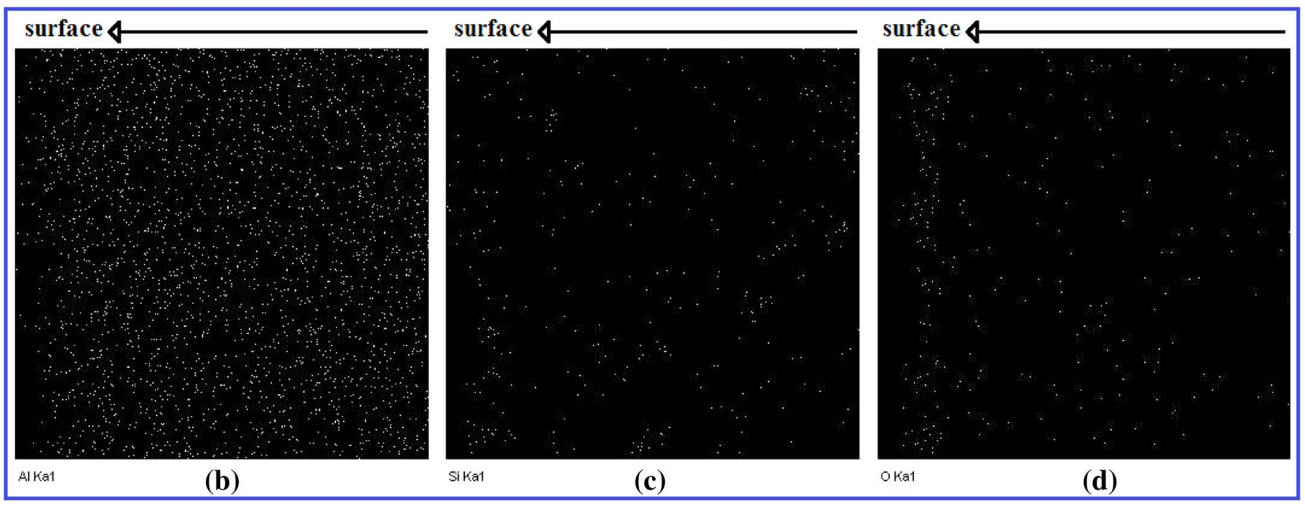

Fig. 9 Map (FE-SEM) results of Alumina–SiC nanocomposite after heat-treatment at 1500 °C for 2 h

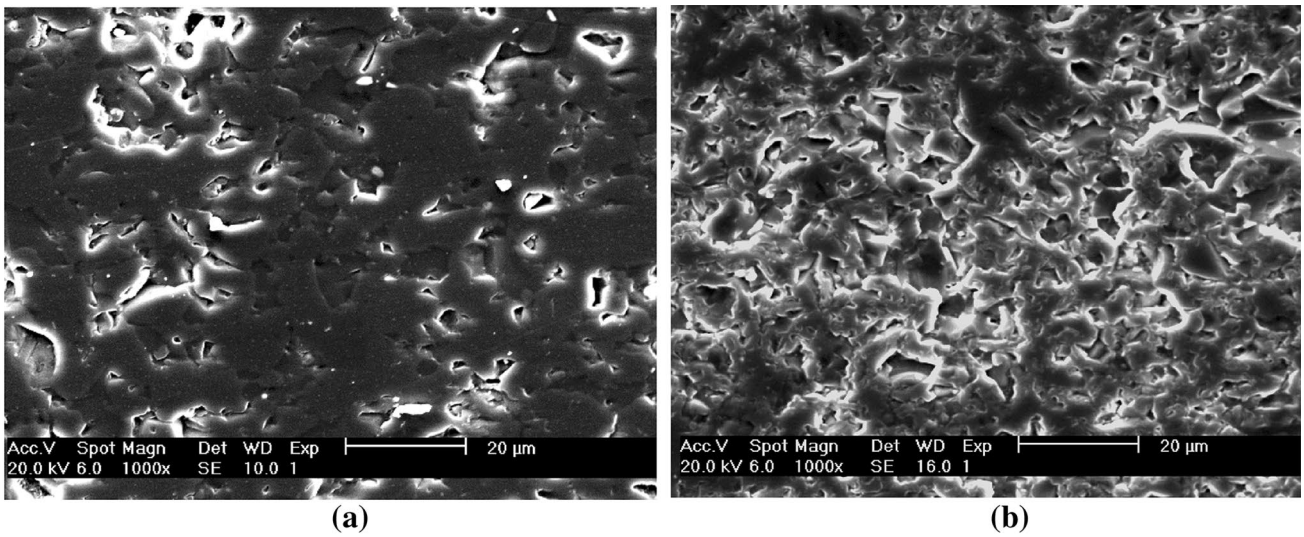

Fig. 10 SEM images of alumina–SiC nanocomposites after heat-treatment for 2 h at **a** 1400 °C and **b** 1500 °C

References

1. D. Galusek, D. Galusková, Alumina matrix composites with non-oxide nanoparticle addition and enhanced functionalities. Nanomaterials **5**(1), 143–143 (2015)
2. J.L. Huang, P.K. Nayak, Strengthening alumina ceramic matrix nanocomposites using spark plasma sintering. Adv Ceram Matrix Composites **2**(1), 247–247 (2018)
3. P. Palmero, Structural ceramic nanocomposites: a review of properties and powders' synthesis methods. Nanomaterials **5**(2), 656–656 (2015)
4. P. M. Ajayan, L. S. Schadler, P. V. Braun, Nanocomposite science and technology, Wiley, 1st edn, 2003
5. Y.L. Dong, F.M. Xu, X.L. Shi, C. Zhang, Z.J. Zhang, J.M. Yang, Y. Tan, Fabrication and mechanical properties of nano-/micro-sized Al_2O_3/SiC composites. Mater. Sci. Eng. A **504**(1–2), 54–54 (2009)
6. G.B. Shan, Y.Z. Chen, M.M. Gong, H. Dong, B. Li, F. Liu, Influence of Al_2O_3 particle pinning on thermal stability of nanocrystalline Fe. J. Mater. Sci. Technol. **34**(4), 604–604 (2018)
7. X.L. Shi, F.M. Xu, Z.J. Zhang, Y.L. Dong, Y. Tan, L. Wang, J.M. Yang, Mechanical properties of hot-pressed Al_2O_3/SiC composites. Mater. Sci. Eng. A **527**(18-19), 4649–4649 (2010)
8. F. Chen, S. Yang, J. Wu, J.A.G. Perez, Q. Shen, J.M. Schoenung, E.J. Lavernia, L. Zhang, Spark plasma sintering and densification mechanisms of conductive ceramics under coupled thermal/electric fields. J. Am. Ceram. Soc. **98**(3), 732–740 (2015)
9. A.A. Gazawi, Microstructure and mechanical properties of aluminum based nanocomposites strengthened with alumina and silicon carbide, pp 152-1, in Ph.D. Thesis, University of Waikato, Hamilton, 2014
10. D. Wang, C. Xue, Y. Cao, J. Zhao, Microstructure design and preparation of Al_2O_3/TiC/TiN micro-nano-composite ceramic tool materials based on properties prediction with finite element method. Ceram. Int. **44**(5), 5101–5101 (2018)
11. M. Parchovianský, D. Galusek, M. Michálek, P. Švanˇcárek, M. Kašiarová, J. Dusza, M. Hnatko, Effect of the volume fraction of SiC on the microstructure and creep behavior of hot pressed Al_2O_3/SiC composites. Ceram. Int. **40**(1), 1807–1814 (2014)
12. A.R. Yazdi, H. Baharvandi, H. Abdizadeh, J. Purasad, A. Fathi, H. Ahmadi, Effect of sintering temperature and silicon carbide fraction on density, mechanical properties and fracture mode of alumina/silicon carbide micro/nano composites. Mater. Des. J. **37**(1), 255–255 (2012)
13. M. Jaafar, G. Bonnefont, G. Fantozzi, H. Reveron, Intergranular alumina–SiC micro-nanocomposites sintered by spark plasma sintering. Mater. Chem. Phys. **124**(1), 379–379 (2010)
14. M. Parchoviansky, D. Galusek, J. Sedlácek, P. Svancárek, M. Kasiarová, J. Dusza, P. Sajgalík, Microstructure and mechanical properties of hot pressed Al_2O_3/SiC nanocomposites, J. Eur. Ceram. Soc. **33** [12] 2298-2291 (2013)
15. F. Surani, H. Abdizadeh, H. Baharvandi, A. Nemati, Effect of MgO nanoparticles on sintering behavior of Al_2O_3–SiC-MgO nanocomposites. Int. Modern Phys J. **5**(1), 573–573 (2012)
16. L.A. Timms, C.B. Ponton, M. Strangewood, Processing of Al_2O_3–SiC Nanocomposite—part 2: green body formation and sintering. J. Eur. Ceram. Soc. **22**(1), 1586–1586 (2002)
17. H.Z. Wang, L. Gao, J.K. Guo, The effect of nano scale SiC particles on the microstructure of Al_2O_3 ceramics, Ceram Int., **26** [4] 396–391 (2000)
18. S.T. Oh, K.I. Tajima, M. Ando, T. Ohji, Strengthening of porous alumina by pulse electric current sintering and nanocomposite processing. J. Am. Ceram. Soc. **83**(5), 1316–1316 (2000)
19. D. Sciti, J. Vicens, A. Bellosi, Microstructure and properties of alumina–SiC nanocomposites prepared from ultrafine powders. J. Mater. Sci. **37**(17), 3758–3758 (2002)
20. T. Osada, W. Nakao, K. Takahashi, K. Ando, Sh Saito, Strength recovery behavior of machined Al_2O_3/SiC nano-composite ceramics by crack-healing. J. Eur. Ceram. Soc. **27**(10), 3267–3267 (2007)
21. H.S. Kim, M.K. Kim, S.B. Kang, S.H. Ahnd, K.W. Namd, Bending strength and crack-healing behavior of Al_2O_3/SiC composites ceramics. Mater. Sci. Eng. A **483**, 675–675 (2008)
22. ASTM B311, Standard test method for density of powder metallurgy (pm) materials containing less than two percent porosity, 2017
23. ASTM C1161, Standard test method for flexural strength of advanced ceramics at ambient temperature, 2018

24. S.P. Liu, K. Ando, B.S. Kim, K. Takahashi, In situ crack-healing behavior of Al_2O_3/SiC composite ceramics under static fatigue strength. Int. Commun. Heat Mass Transfer **36**, 563–563 (2009)
25. Z. Wang, S. Wang, X. Zhang, P. Hu, W. Han, C. Hong, Effect of graphite flake on microstructure as well as mechanical properties and thermal shock resistance of ZrB_2–SiC matrix ultrahigh temperature ceramics. J Alloys Compd **4**(1–2), 484–484 (2009)
26. X.H. Zhang, Z. Wang, P. Hu, W.B. Han, C.Q. Hong, Mechanical properties and thermal shock resistance of ZrB2–SiC ceramic toughened with graphite flake and SiC whiskers. Scripta Mater. **61**(8), 812–812 (2009)
27. O.T. Johnson, P. Rokebrand, I. Sigalas, Microstructure and properties of Al2O3–SiC. Proceedings of the World Congress on Engineering, London, UK, 2014
28. X. Sun, J.G. Li, S. Guo, Z. Xiu, K. Duan, X.Z. Hu, Intragranular particle residual stress strengthening of Al_2O_3–SiC nanocomposites. J. Am. Ceram. Soc. **88**(8), 1543–1543 (2005)
29. N. Saheb, K. Mohammad, Microstructure and mechanical properties of spark plasma sintered Al_2O_3–SiC–CNTs hybrid nanocomposites. Ceram. Int. **42**(10), 12340–12340 (2016)

Publisher's Note Springer Nature remains neutral with regard to jurisdictional claims in published maps and institutional affiliations.